

# High-Field Chlorine NMR Spectroscopy of Solid Organic Hydrochloride Salts: A Sensitive Probe of Hydrogen Bonding Environment

David L. Bryce,<sup>†‡</sup> Myrlene Gee,<sup>†‡</sup> and Roderick E. Wasylshen<sup>\*‡</sup>

Department of Chemistry, Dalhousie University, Halifax, Nova Scotia, Canada B3H 4J3, and  
Department of Chemistry, University of Alberta, Edmonton, Alberta, Canada T6G 2G2

Received: May 22, 2001

A series of organic hydrochloride salts has been investigated using solid-state  $^{35}\text{Cl}$  and  $^{37}\text{Cl}$  NMR spectroscopy at applied magnetic field strengths of 9.4 and 18.8 T. Magic-angle spinning, static Hahn-echo, and quadrupolar Carr–Purcell Meiboom–Gill (QCPMG) echo experiments have been applied to investigate the chlorine electric field gradient (EFG) and chemical shift (CS) tensors for L-tyrosine hydrochloride, L-cysteine methyl ester hydrochloride, L-cysteine ethyl ester hydrochloride, quinuclidine hydrochloride, and tris sarcosine calcium chloride. Chlorine-35 nuclear quadrupolar coupling constants for these compounds range from 2.23 to 5.25 MHz, and isotropic chemical shifts range from approximately 9 to 53 ppm relative to the chloride ion in aqueous solution. The results demonstrate the feasibility and benefits of high-field  $^{35/37}\text{Cl}$  NMR studies of organic chloride salts. A discussion of the data in the context of the known X-ray or neutron diffraction structures for these compounds suggests that the chlorine EFG tensor is a valuable probe of hydrogen bonding to the chloride ion. Because the anisotropies of the CS tensors are rather small, precise determination of the chlorine CS tensors proved to be challenging and was only feasible for L-cysteine ethyl ester hydrochloride, where the span,  $\Omega$ , was found to be  $47 \pm 4$  ppm. This represents the first determination of  $\Omega(\text{Cl})$  from a powder sample. Results of ab initio calculations of the chlorine EFG and CS tensors in L-tyrosine hydrochloride are presented and compared with the experimental data.

## Introduction

The increasing accessibility of high-field NMR spectrometers (17.6 T, 18.8 T, and beyond) has opened up the possibility of studying hitherto relatively inaccessible nuclei. For solid samples, half-integer spin quadrupolar nuclei benefit greatly from high applied magnetic field strengths due to the inverse relationship between the second-order quadrupolar broadening and  $B_0$ .<sup>1–3</sup> Indeed, high applied magnetic fields make possible the study of nuclei with low magnetogyric ratios,  $\gamma$ , which simply are not feasible at moderate field strengths. Chlorine has two NMR-active isotopes,  $^{35}\text{Cl}$  ( $I = 3/2$ ; N. A. = 75.53%;  $\gamma = 2.6242 \times 10^7 \text{ rad T}^{-1} \text{ s}^{-1}$ ;  $Q = -82 \text{ mb}^4$ ) and  $^{37}\text{Cl}$  ( $I = 3/2$ ; N. A. = 24.47%;  $\gamma = 2.1844 \times 10^7 \text{ rad T}^{-1} \text{ s}^{-1}$ ;  $Q = -64.6 \text{ mb}^{4c,5}$ ). The relatively low values of  $\gamma$  and moderately large quadrupole moments for these nuclei make them excellent candidates for high-field NMR studies. Smith has recently reviewed the progress made in solid-state NMR of low- $\gamma$  nuclei and has summarized the available solid-state NMR parameters for  $^{35}\text{Cl}$ .<sup>2</sup> To date, single-crystal  $^{35}\text{Cl}$  NMR studies have been carried out on  $\text{NaClO}_3$ ,<sup>6</sup>  $\text{Mn}(\text{CO})_5\text{Cl}$ ,<sup>7</sup> tris sarcosine calcium chloride,<sup>8</sup>  $\text{NH}_4\text{ClO}_4$ ,<sup>9</sup> and betaine calcium chloride dihydrate.<sup>10</sup> Perchlorate anions have been a popular focus of chlorine solid-state NMR studies due to the high local symmetry at chlorine.<sup>11–16</sup> Studies of inorganic chlorides have been reported,<sup>17–23</sup> in many cases, such as the alkali metal chlorides, the chlorine nuclear quadrupolar coupling constant is zero due to cubic symmetry. A limited number of organic or ammonium hydrochloride salts

have been studied previously:  $\text{NH}_4\text{Cl}$ ,<sup>18</sup>  $\text{C}_4\text{H}_9\text{NH}_3\text{Cl}$ ,<sup>24</sup> and cocaine hydrochloride.<sup>25</sup>

Due to large quadrupolar coupling constants, NMR studies of compounds with covalently bound chlorine atoms are difficult in solution due to extremely efficient nuclear spin relaxation, and are untenable in the solid state using conventional pulsed FT techniques owing to extremely broad line shapes. Conversely, nuclear quadrupole resonance (NQR) methods<sup>26</sup> are difficult to apply when chlorine nuclei are in high-symmetry environments. Furthermore, they do not allow one to characterize the chlorine magnetic shielding tensors. Oxychloro and chloride anions, therefore, represent an appealing situation for  $^{35/37}\text{Cl}$  solid-state NMR, where the high local symmetry guarantees relatively small quadrupolar coupling constants. The most insightful chlorine solid-state NMR study to date is that of Skibsted and Jakobsen.<sup>16</sup> This study focuses on the chlorine NMR interaction tensors of the perchlorate anion in several inorganic perchlorates and establishes chlorine solid-state NMR as a viable and informative technique for the investigation of these types of materials. Their experiments show that the chlorine chemical shifts for a wide variety of perchlorate salts fall in the narrow range of  $\sim 980$  to 1005 ppm relative to  $\text{NaCl}(\text{aq})$  and that the  $^{35}\text{Cl}$  nuclear quadrupolar coupling constants range from 0.3 to 3.0 MHz.

In the present work, we demonstrate the feasibility and utility of high-field chlorine NMR studies of solid organic hydrochloride salts. Chlorine NMR spectroscopy of such compounds represents an excellent probe of the local chlorine environment since any deviations from perfect cubic symmetry at chlorine will result in an observable quadrupolar coupling constant. In particular, Yesinowski et al. have remarked upon the potential

\* To whom correspondence should be addressed. Phone: 780-492-4336. Fax: 780-492-8231. Email: Roderick.Wasylshen@UAlberta.ca

<sup>†</sup> Dalhousie University.

<sup>‡</sup> University of Alberta.

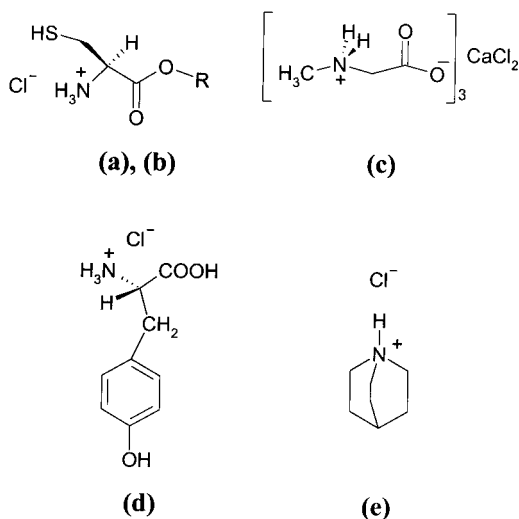


**Figure 1.** Simple structural representations of the hydrochloride salts investigated in the present work: (a) L-cysteine methyl ester hydrochloride ( $R = \text{Me}$ ); (b) L-cysteine ethyl ester hydrochloride ( $R = \text{Et}$ ); (c) tris sarcosine calcium chloride; (d) L-tyrosine hydrochloride; (e) quinuclidine hydrochloride.

application of high-field NMR techniques to investigate the relationship between the chlorine nuclear quadrupolar coupling tensor and the hydrogen bonding environment about chlorine in organic hydrochlorides.<sup>25</sup> We explore this relationship by comparing the  $^{35}\text{Cl}$  NMR parameters to known crystal structures for the following set of compounds in which chloride anions exist in a variety of hydrogen-bonding environments (Figure 1): L-tyrosine hydrochloride,<sup>27</sup> L-cysteine methyl ester hydrochloride,<sup>28</sup> L-cysteine ethyl ester hydrochloride,<sup>28</sup> quinuclidine hydrochloride,<sup>29</sup> and tris sarcosine calcium chloride.<sup>30</sup> The  $^{35}\text{Cl}$  and  $^{37}\text{Cl}$  electric field gradient (EFG) and chemical shift (CS) tensors are examined using a variety of experimental techniques at 9.4 and 18.8 T, including magic-angle spinning (MAS) NMR, Hahn-echo spectroscopy<sup>31,32</sup> on stationary samples, and, for some compounds, quadrupolar Carr–Purcell Meiboom–Gill (QCPMG) or “spikelet echo” spectroscopy<sup>33–38</sup> on stationary samples. The principal benefit of the latter experiment is that it provides an order of magnitude enhancement in the signal-to-noise relative to standard static echo methods. Ab initio methods for the calculation of chlorine NMR interaction tensors for the chloride anion in a hydrogen-bonded environment are employed to provide additional insight into the experimental results.

## Theory and Background

The pertinent interactions for an isolated half-integer spin quadrupolar nucleus such as  $^{35}\text{Cl}$  have been presented.<sup>1</sup> To avoid undue repetition, we refer the interested reader to our recent solid-state  $^{11}\text{B}$  and  $^9\text{Be}$  NMR studies, which provide a summary of the relevant equations and definitions.<sup>39,40</sup> Briefly, the Zeeman, quadrupolar, and nuclear magnetic shielding interactions will influence the spectrum of an isolated spin-3/2 nucleus in a stationary powdered sample. Here, we focus our discussion on the central  $1/2 \leftrightarrow -1/2$  transition since it is not perturbed by the first-order quadrupolar interaction. Under conditions of MAS, the nuclear magnetic shielding tensor ( $\sigma$ ) is averaged to its isotropic value,  $\sigma_{\text{iso}}$ . The second-order quadrupolar interaction will dominate the observed line shape and modify the apparent isotropic chemical shift such that the observed “center-of-gravity” shift is a sum of the true isotropic chemical shift and a second-order quadrupolar shift.<sup>41</sup> Since different conventions exist for reporting NMR parameters, some of the definitions

for the parameters discussed in the present work are provided below to avoid confusion.

According to the conventions established in reference 42, the principal components of the symmetric part of the CS tensor are designated and ordered as  $\delta_{11} \geq \delta_{22} \geq \delta_{33}$  and the span of the nuclear magnetic shielding or CS tensor is defined as

$$\Omega = \sigma_{33} - \sigma_{11} \approx \delta_{11} - \delta_{33} \quad (1)$$

The skew of the tensors is defined as<sup>42</sup>

$$\kappa = \frac{3(\sigma_{\text{iso}} - \sigma_{22})}{\Omega} \approx \frac{3(\delta_{22} - \delta_{\text{iso}})}{\Omega} \quad (2)$$

The components of the EFG tensor in its principal axis system are defined and ordered as

$$|V_{zz}| \geq |V_{yy}| \geq |V_{xx}| \quad (3)$$

and the quadrupolar coupling constant,  $C_Q$ , is given by

$$C_Q = \frac{eQV_{zz}}{h} \quad (4)$$

where  $e$  is the charge of an electron and  $Q$  is the nuclear quadrupole moment. The asymmetry parameter,  $\eta$ , is defined as

$$\eta = \frac{V_{xx} - V_{yy}}{V_{zz}} \quad (5)$$

The theory relating to solid-state QCPMG experiments has been described in reference 35.

## Experimental Section

**(i) Sample Preparation.** Crystals of tris sarcosine calcium chloride were obtained from an aqueous solution of sarcosine and  $\text{CaCl}_2$  by slow evaporation as described by Ashida et al.<sup>30</sup> The identity and purity of the product were confirmed by  $^{13}\text{C}$  CP/MAS NMR. L-Cysteine methyl ester hydrochloride, L-cysteine ethyl ester hydrochloride, and quinuclidine hydrochloride were purchased from Sigma-Aldrich and used without further purification. For all of the compounds studied, X-ray or neutron diffraction studies<sup>27–30</sup> indicate that there is only one chlorine site and all spectra were analyzed as such. Compounds were powdered and packed into rotors for solid-state NMR spectroscopy.

**(ii) Solid-State NMR Spectroscopy.** Chlorine-35 solid-state NMR spectra were obtained on Varian Inova ( $B_0 = 18.8$  T,  $\nu_L(^{35}\text{Cl}) = 78.36$  MHz) and Bruker AMX ( $B_0 = 9.4$  T,  $\nu_L(^{35}\text{Cl}) = 39.18$  MHz) spectrometers. A mid-bore (63 mm) Doty CP/MAS triple resonance probe, with 5 mm (o.d.) rotors, was used on the Varian system; MAS rates of up to 15 kHz were used. A wide-bore (72 mm) Bruker low-band probe was used on the AMX spectrometer with 7 mm (o.d.) rotors; MAS rates greater than 4 kHz were not practical on this system. High-power proton decoupling was used on the 18.8 T system only. Experiments were set up using solid sodium chloride. The “solid”  $\pi/2$  pulse was 5.75  $\mu\text{s}$  on the 18.8 T system and 4.5  $\mu\text{s}$  on the 9.4 T system. In practice, shorter pulse widths were sometimes used to provide more uniform excitation of the spectra. The magic angle was calibrated on the satellite transitions of the  $^{35}\text{Cl}$  resonance of solid NaCl. Due to broad signals and to avoid interference from probe ringing, echoes ( $\pi/2 - \tau_1 - \pi - \tau_2$ ) were used for both stationary and MAS samples. QCPMG or spikelet

echo experiments were carried out using the pulse sequence given in refs 35 and 38. Briefly, we may summarize this sequence as:  $(\pi/2)_x - \tau_1 - (\pi)_y - \tau_2 - \text{ACQ} - [\tau_3 - (\pi)_y - \tau_4 - \text{echo}]^M - \tau_d$ , where the echoes are sampled in the period marked "echo". Phase cycling requirements are given in ref 35. Typically,  $M = 32$  repeating units were used and the number of points acquired was adjusted so that the sideband separation was 1–10 kHz. Left shifting of the FID prior to FT was typically used for all spectra except the QCPMG spectra, where acquisition exactly at the top of the echo is critical for obtaining reliable spectra. Recycle delays were 0.4–0.5 s for all compounds. Chlorine-37 NMR spectra were obtained on the Bruker instrument ( $B_0 = 9.4$  T,  $\nu_L(^{37}\text{Cl}) = 32.63$  MHz) with pulse widths of 2.75  $\mu\text{s}$ . The  $^{37}\text{Cl}$  NMR spectra were used in combination with the  $^{35}\text{Cl}$  NMR spectra to refine the quadrupolar tensor parameters reported herein. All spectra were processed using VNMR,<sup>43</sup> NUTS,<sup>44</sup> and WINNMR.<sup>45</sup> Gaussian line broadening functions of 200–1000 Hz were applied to spectra of stationary samples, 50–150 Hz to spectra of MAS samples, and 20–70 Hz to QCPMG spectra.

Experimentally, spectra were referenced to the chlorine resonance of NaCl(s) at 0.00 ppm. The following relationships were employed to convert the chemical shifts so that they are with respect to the primary reference, an infinitely dilute solution of NaCl in  $\text{H}_2\text{O}$ . The chemical shift of NaCl(s) with respect to KCl(s) is  $-49.73$  ppm.<sup>46</sup> The chemical shift of KCl(s) with respect to 1 M NaCl in  $\text{H}_2\text{O}$  is 3.90 ppm.<sup>46</sup> Finally, the chemical shift of 1 M NaCl(aq) with respect to an infinitely dilute NaCl solution in  $\text{H}_2\text{O}$  is about  $-0.51$  ppm.<sup>47</sup> Thus the conversion factor is (see Note Added in Proof):

$$\delta \text{ (rel. to NaCl in } \text{H}_2\text{O, inf. dilute)} = \delta \text{ (rel. to NaCl(s))} - 46.34 \text{ ppm} \quad (6)$$

The chemical shift values reported in this paper are with respect to infinitely dilute NaCl in  $\text{H}_2\text{O}$  at 0.00 ppm. It should be noted that the  $^{35}\text{Cl}$  chemical shifts for the chloride ion in  $\text{H}_2\text{O}$  compared with  $\text{D}_2\text{O}$  are significantly different.<sup>48</sup> The spectra shown in Figures 2–5 (scale in kHz) are with respect to solid NaCl at 0.0 kHz.

Most spectra were simulated using the WSOLIDS software package,<sup>49</sup> which incorporates the space-tiling algorithm of Alderman et al.<sup>50</sup> QCPMG spectra were simulated using the SIMPSON program.<sup>51</sup> The QCPMG simulations take into account the possibility of incomplete or nonuniform spectral excitation by considering experimental parameters such as the finite pulse widths and rf field strength used.

**(iii) Ab Initio Calculations.** Calculations of chlorine electric field gradient and nuclear magnetic shielding tensors were done using Gaussian 98 and Gaussian 98W<sup>52</sup> running on an IBM RS/6000 workstation with dual 200 MHz processors and a Dell Dimension PC (Pentium III, 550 MHz, 128 Mb RAM). The geometry of ammonium chloride was taken from the solid-state neutron diffraction structure,<sup>53</sup> with  $r(\text{N}-\text{H})$  equal to 1.03 Å and an equilibrium nitrogen–chlorine distance of 1.933 Å. The geometry of sodium perchlorate used in the calculations employed a tetrahedral  $\text{ClO}_4^-$  moiety with Cl–O bond lengths of 1.42 Å and a chlorine–sodium equilibrium internuclear distance of 3.54 Å,<sup>54,55</sup> where the sodium atom lies in one of the O–Cl–O planes and bisects the O–Cl–O angle (model A from ref 54). The gas-phase equilibrium sodium–chlorine distance in NaCl is 2.3608 Å.<sup>56</sup> The geometry of L-tyrosine hydrochloride was constructed from the neutron diffraction atomic coordinates,<sup>27</sup> vide infra. Calculations of nuclear magnetic shielding tensors were done using the GIAO (gauge-

independent atomic orbitals) method.<sup>57</sup> Locally dense basis sets<sup>58</sup> were used in some cases. All basis sets (3-21G, 6-311G, 6-311+G\*, 6-311++G\*\*) were available within the Gaussian package. The nuclear quadrupolar coupling constants,  $C_Q$ , were determined from the calculated largest EFG component,  $V_{ZZ}$ , by means of eq 4. Conversion of  $V_{ZZ}$  from atomic units to  $\text{Vm}^{-2}$  was carried out by using the factor  $9.7177 \times 10^{21} \text{ Vm}^{-2}$  per atomic unit.<sup>59</sup> It should be noted that Gaussian 98 reports  $V_{ZZ}$  with sign opposite to the convention used in eq 4; Gaussian output was corrected for this. The accepted value of the nuclear quadrupole moment,  $Q$ , for  $^{35}\text{Cl}$  is  $-82 \text{ mb}$ .<sup>4</sup> The ratio  $Q(^{37}\text{Cl})/Q(^{35}\text{Cl})$  is known to be 0.7880983,<sup>4c,5</sup> and so  $Q(^{37}\text{Cl})$  is  $-64.6 \text{ mb}$ .

Calculated nuclear magnetic shielding tensors were converted to chemical shift tensors using the absolute shielding scale for chlorine.<sup>47</sup> The absolute shielding constant for the primary reference, an infinitely dilute aqueous solution of NaCl, is  $974 \pm 4$  ppm. Therefore, calculated shielding constants were converted to chemical shifts via the following equation:

$$\delta = 974 - \sigma \quad (7)$$

where all quantities are in ppm.

## Results and Discussion

**(i)  $^{35}\text{Cl}$  NMR Spectra with MAS.** Acquisition of  $^{35}\text{Cl}$  MAS spectra of the  $1/2 \leftrightarrow -1/2$  transition of compounds containing chloride ions with quadrupolar coupling constants of less than 4 MHz was straightforward on the 18.8 T magnet at MAS rates of 10–15 kHz. Signals were easily observed after a single scan. Spectra with well-defined second-order quadrupolar line shapes and good signal-to-noise ratios were generally obtained in approximately 30 min. Shown in Figure 2 are central transition spectra of MAS samples of (a) L-cysteine ethyl ester hydrochloride, (b) L-cysteine methyl ester hydrochloride, and (c) L-tyrosine hydrochloride. The best-fit parameters for the simulated spectra are given in Table 1. The  $^{35}\text{Cl}$  quadrupolar coupling constant for this series of compounds ranges from approximately 2 to 4 MHz, and the quadrupolar asymmetry parameter ranges from nearly zero to greater than 0.8. Conversely, the isotropic chemical shifts are fairly constant, all falling between 45 and 55 ppm. This small variation in the chemical shift is also found for perchlorate salts,<sup>16</sup> although the chemical shift ranges for the two classes of compounds are on the order of 1000 ppm apart. The variation in chemical shifts within either class of compounds, on the order of tens of ppm, represents less than 5% of the total known chemical shift range for chlorine, 1500 ppm.<sup>60,61</sup> The variation in  $C_Q$ , which has been measured for both the hydrochloride salts and the perchlorates, is also relatively small,  $< 5\%$ , since values of up to  $-150 \text{ MHz}$  are known.<sup>47,62</sup> A more complete discussion of the dependence and sensitivity of the chlorine NMR interaction tensors on the local environment, in particular the hydrogen bonding about chlorine, is presented below. To our knowledge, the spectra presented in Figure 2 are the first that explicitly demonstrate via sharp second-order line shapes the potential of  $^{35}\text{Cl}$  MAS solid-state NMR for the study of organic hydrochloride salts. It is important to recognize that local sample heating induced by MAS is likely to slightly alter the chlorine nuclear quadrupolar coupling constant from that determined from a stationary sample.

Given the range of chlorine quadrupolar coupling constants determined using MAS NMR for chloride anions, 2 to 4 MHz, multiple-quantum MAS (MQMAS) experiments<sup>63</sup> on  $^{35/37}\text{Cl}$  nuclei should be practical at high field strengths for identifying and characterizing nonequivalent chlorine sites in these types

**TABLE 1: Summary of  $^{35}\text{Cl}$  NMR Parameters for the Organic Hydrochloride Salts Investigated**

molecule	$C_Q/\text{MHz}$	$\eta$	$\delta_{\text{iso}}/\text{ppm}$	$\Omega/\text{ppm}$	$\kappa$
L-tyrosine $\text{HCl}^a$	$2.23 \pm 0.02$	$0.72 \pm 0.03$	$49.3 \pm 0.5$	$< 150$	
L-cysteine methyl ester $\text{HCl}^a$	$2.37 \pm 0.01$	$0.81 \pm 0.03$	$48.2 \pm 0.7$	$45 \pm 15$	
L-cysteine ethyl ester $\text{HCl}^b$	$3.78 \pm 0.02$	$0.03 \pm 0.03$	$53.2 \pm 0.5$	$47 \pm 4$	$-0.8 \pm 0.2$
tris sarcosine $\text{CaCl}_2^c$	$4.04 \pm 0.03$	$0.62 \pm 0.02$	$14.7 \pm 10.0$	$< 150$	
quinuclidine $\text{HCl}^c$	$5.25 \pm 0.02$	$0.05 \pm 0.01$	$9.7 \pm 10.0$	$50 \pm 20$	

<sup>a</sup> Parameters determined from MAS and static Hahn-echo  $^{35}\text{Cl}$  spectra acquired at 18.8 T. <sup>b</sup> Parameters determined from MAS, Hahn-echo, and QCPMG  $^{35}\text{Cl}$  spectra acquired at 18.8 T. <sup>c</sup> Parameters determined from Hahn-echo  $^{35}\text{Cl}$  spectra acquired at 18.8 and 9.4 T, and Hahn-echo  $^{37}\text{Cl}$  spectra acquired at 9.4 T.

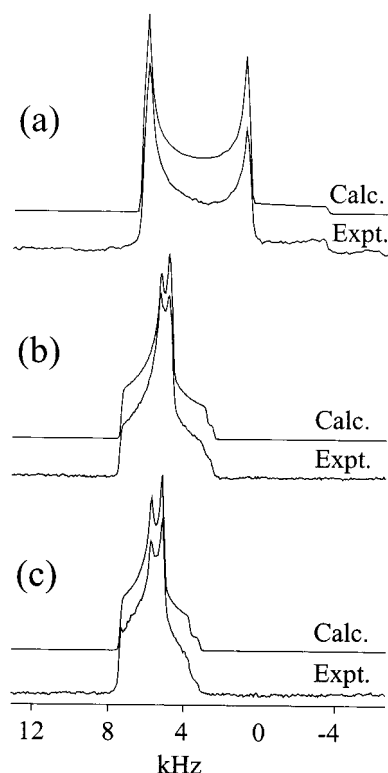


**Figure 2.** Experimental and calculated central transition region of the high-field ( $B_0 = 18.8$  T)  $^{35}\text{Cl}$  NMR spectra of magic-angle spinning powder samples of (a) L-cysteine ethyl ester hydrochloride ( $\nu_{\text{rot}} = 13.6$  kHz); (b) L-cysteine methyl ester hydrochloride ( $\nu_{\text{rot}} = 14.2$  kHz); (c) L-tyrosine hydrochloride ( $\nu_{\text{rot}} = 14.8$  kHz). Best-fit parameters are given in Table 1.

of compounds. Standard MAS and SATRAS<sup>64,65</sup> experiments have already proven to be effective in the identification and characterization of multiple perchlorate sites exhibiting very small quadrupolar coupling constants, e.g., the two unique sites in  $\text{Mg}(\text{ClO}_4)_2 \cdot 6\text{H}_2\text{O}$  have  $C_Q(^{35}\text{Cl})$  values of 0.309 and 0.475 MHz.<sup>16</sup>

(ii)  $^{35/37}\text{Cl}$  NMR Spectra of Stationary Samples. While MAS spectra allow for the characterization of the chlorine EFG tensor, analysis of the chlorine NMR spectra of stationary samples has the potential to provide information concerning the chemical shift tensor, i.e., its principal components and its orientation with respect to the EFG tensor. For the majority of the compounds studied herein, quantitative characterization of the chlorine chemical shift tensor proved to be difficult even at 18.8 T. This is simply due to the fact that the span of the chemical shift tensor typically amounts only to a few kHz (e.g.,  $50 \text{ ppm} \times 78.3 \text{ Hz ppm}^{-1} = 3.9 \text{ kHz}$ ), while the central transition spectra predicted based solely upon the quadrupolar interaction may be as wide as 100 kHz. However, for L-cysteine ethyl ester hydrochloride, a quantitative determination of the chlorine chemical shift tensor was possible. Shown in Figure 3 are experimental and simulated Hahn-echo and QCPMG  $^{35}\text{Cl}$

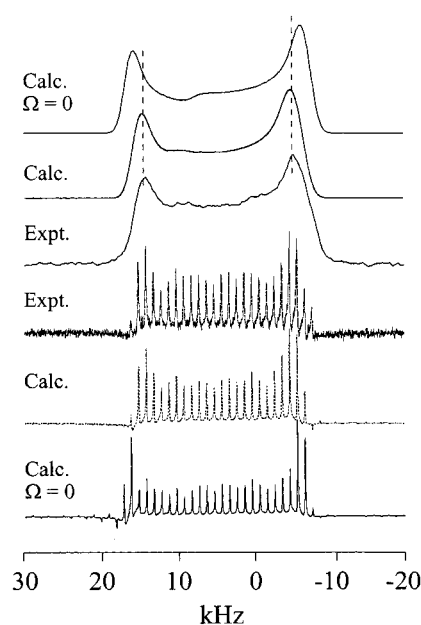


**Figure 3.** Experimental  $^{35}\text{Cl}$  NMR static echo (top) and QCPMG (bottom) spectra of L-cysteine ethyl ester hydrochloride,  $B_0 = 18.8$  T, along with the best-fit simulated spectra. Also shown are simulated spectra for which a span of zero was used. Spikelets in the QCPMG spectra are spaced at 1 kHz intervals.

spectra of L-cysteine ethyl ester hydrochloride, for which the chlorine CS tensor was determined to have a span of  $47 \pm 4$  ppm and a skew of  $-0.8 \pm 0.2$  (Table 1). This corresponds to principal components of  $\delta_{11} = 83$ ,  $\delta_{22} = 41$ , and  $\delta_{33} = 36$  ppm. Additionally, the simulations indicate that the largest components of the EFG and nuclear magnetic shielding tensors ( $V_{ZZ}$  and  $\sigma_{33}$ ) are at  $90^\circ$  with respect to one another. The simulation of the QCPMG spectrum is comparable to those where anisotropic chemical shift information has been extracted previously, e.g.,  $^{87}\text{Rb}$  spectra of  $\text{RbClO}_4$  and  $\text{RbVO}_3$  and  $^{59}\text{Co}$  spectra of  $(\text{Co}(\text{NH}_3)_5\text{Cl})\text{Cl}_2$ .<sup>35</sup> Although they are acquired at the same magnetic field strength, simulations of the QCPMG spectrum and the Hahn-echo spectrum in combination were useful to refine and establish accurately the EFG and CS parameters. Simulations of Hahn-echo and QCPMG spectra of L-tyrosine hydrochloride and L-cysteine methyl ester hydrochloride (not shown) did not allow for a precise determination of the chlorine chemical shift tensor in these compounds. Estimated limits on the span of the chlorine CS tensors are given in Table 1.

While reports on the chlorine EFG tensor in organic hydrochlorides are scarce,<sup>2,24,25</sup> information concerning the chlorine chemical shift tensor in such compounds is virtually nonexistent. Even isotropic chemical shifts are rare for solid hydrochloride salts. We may, however, compare the span of 47 ppm in L-cysteine ethyl ester hydrochloride to two known chlorine chemical shift tensor spans of oxychloro anions, both determined from single-crystal  $^{35}\text{Cl}$  studies:  $\Omega = 32.0 \pm 1.2$  ppm for  $\text{NH}_4\text{ClO}_4$ ,<sup>9</sup> and  $\Omega = 40 \pm 7$  ppm for  $\text{NaClO}_3$ .<sup>6</sup> The



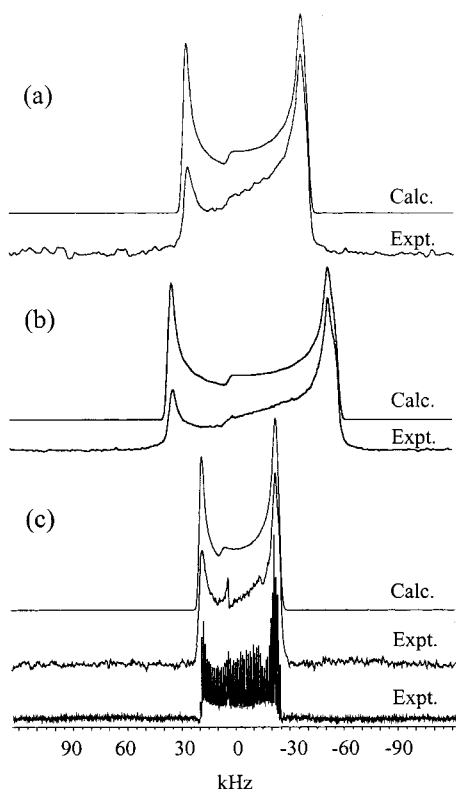


**Figure 4.** Experimental chlorine NMR static echo spectra of quinuclidine hydrochloride acquired for (a)  $^{37}\text{Cl}$  at 9.4 T, (b)  $^{35}\text{Cl}$  at 9.4 T, and (c)  $^{35}\text{Cl}$  at 18.8 T, along with the best-fit simulations. Also shown in part (c) is the experimental  $^{35}\text{Cl}$  QCPMG spectrum acquired at 18.8 T. The experimental spectra shown in parts (a) and (b) suffer from nonuniform excitation across the  $\sim 100$  kHz breadth. The sharp feature at 4.1 kHz in part (c) is the isotropic resonance due to a small amount of solvated quinuclidine hydrochloride in the sample.

total range of chloride ion chemical shifts for the compounds studied in the present work is less than 50 ppm. It is known from solution NMR studies that chlorine chemical shifts of chloride ions cover a fairly narrow range ( $\sim 30$  ppm) near zero ppm.<sup>60</sup> Given that shielding constants for the chloride ion cover a fairly small range and lie within  $\sim 200$  ppm of the diamagnetic free atom shielding for chlorine (1149 ppm<sup>66</sup>), it is likely that the chloride magnetic shielding tensor is dominated by the diamagnetic contribution; it is therefore reasonable to expect small shielding tensor spans.

Experimental and simulated chlorine Hahn-echo spectra of stationary samples of quinuclidine hydrochloride and tris sarcosine calcium chloride are shown in Figures 4 and 5, respectively. In part (a) of each figure, the  $^{37}\text{Cl}$  spectrum acquired at 9.4 T is shown; parts (b) and (c) show the  $^{35}\text{Cl}$  spectra acquired at 9.4 and 18.8 T. Also shown in the experimental QCPMG spectrum for quinuclidine hydrochloride. All of the spectra acquired at 9.4 T suffer to a certain extent from nonuniform rf excitation; nevertheless, fitting of the discontinuities in the spectra allows for the determination of  $C_Q$  and  $\eta$ . NMR of the  $^{37}\text{Cl}$  nucleus affords narrower line shapes due to its smaller quadrupole moment relative to  $^{35}\text{Cl}$ ; however, the lower natural abundance of  $^{37}\text{Cl}$  results in spectra with lower signal-to-noise ratios relative to  $^{35}\text{Cl}$ . Analyses of both  $^{37}\text{Cl}$  and  $^{35}\text{Cl}$  NMR spectra allow for more accurate and precise determinations of the EFG tensor parameters (Table 1). In Figure 4c, the QCPMG sidebands were deliberately spaced at relatively small (1 kHz) intervals about the transmitter frequency to faithfully mimic the envelope of the powder pattern obtained using a simple Hahn echo pulse sequence.

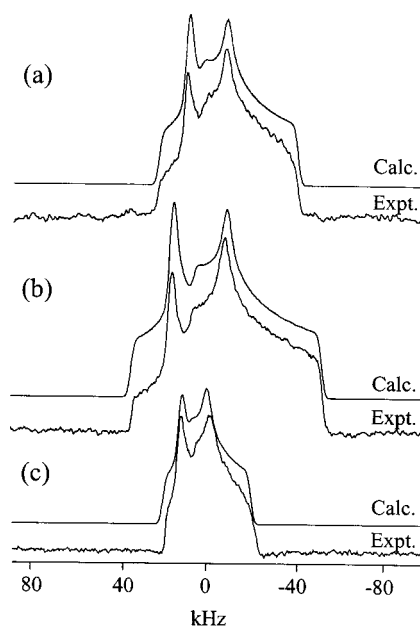


**Figure 5.** Experimental chlorine NMR static echo spectra of tris sarcosine calcium chloride acquired for (a)  $^{37}\text{Cl}$  at 9.4 T, (b)  $^{35}\text{Cl}$  at 9.4 T, and (c)  $^{35}\text{Cl}$  at 18.8 T, along with the best-fit simulations. The experimental spectra shown in parts (a) and (b) suffer from nonuniform excitation across the  $\sim 80$  kHz breadth. An isotropic chemical shift tensor is assumed in the simulations shown. The effects of neglecting anisotropic magnetic shielding are more evident at 18.8 T (part (c)).

To our knowledge, the  $^{35}\text{Cl}$  quadrupolar coupling constant in quinuclidine hydrochloride, 5.25 MHz, is the largest determined directly by chlorine nuclear magnetic resonance spectroscopy to date. A comparable value, 5.027 MHz, has been determined for cocaine hydrochloride.<sup>25</sup> Certainly NQR spectroscopy has been used to determine much larger quadrupolar coupling constants,<sup>26</sup> e.g.,  $C_Q(^{35}\text{Cl})$  in 1,2,4,5-tetrachloro-3,6-dinitrobenzene is 76.937 MHz<sup>67</sup> and  $C_Q(^{35}\text{Cl})$  in solid  $\text{Cl}_2$  at 0 K is 108.975 MHz.<sup>68</sup> A value of  $-145.87$  MHz has been determined by molecular beam electric resonance spectroscopy for the ground vibrational state of gaseous  $\text{ClF}$ .<sup>62</sup> Large  $C_Q$  values may also be determined indirectly by solid-state NMR methods. For example, residual spin-spin interactions between  $^{35}\text{Cl}$  and  $^{13}\text{C}$  in chloroketosulfones have been exploited to determine a  $C_Q(^{35}\text{Cl})$  of  $-73$  MHz.<sup>69</sup>

The chlorine isotropic chemical shifts for tris sarcosine calcium chloride and quinuclidine hydrochloride are identical within error, 9–15 ppm, but significantly different from those determined for L-tyrosine hydrochloride and the L-cysteine alkyl ester hydrochlorides. The neglect of anisotropy in the chlorine chemical shift tensor only becomes apparent in the spectra acquired at 18.8 T. For example, a span of 50 ppm was incorporated into the simulated spectrum of quinuclidine hydrochloride in order to achieve the best fit (Figure 4c), although attempts at fitting this spectrum indicate that there is more than one solution. An isotropic chemical shift tensor was used in the simulated spectrum of tris sarcosine hydrochloride at 18.8 T (Figure 5c); deviations from the experimental spectrum that are clearly different and distinct from those arising due to nonuniform excitation of the powder pattern (i.e., differences in the positions of the discontinuities rather than intensity differences) are apparent.

A single-crystal  $^{35}\text{Cl}$  NMR study of tris sarcosine calcium chloride at 280 K<sup>8</sup> as well as an NQR study of a powder sample at 292 K<sup>70</sup> are available for comparison with our high-field NMR results determined from a powder sample at ambient temperature

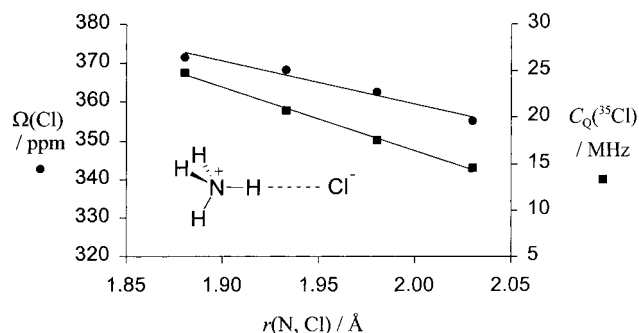


**Figure 6.** Ab initio chlorine chemical shift tensor spans (●) and  $^{35}\text{Cl}$  quadrupolar coupling constants (■) for ammonium chloride as a function of the nitrogen–chlorine separation,  $r(\text{N}, \text{Cl})$ . Trendlines were determined by linear regression to have slopes of  $-111 \text{ ppm } \text{\AA}^{-1}$  (span, ●) and  $-73 \text{ MHz } \text{\AA}^{-1}$  ( $C_Q(^{35}\text{Cl})$ , ■). The equilibrium value of  $r(\text{N}, \text{Cl})$  is  $1.933 \text{ \AA}$ .

( $\sim 276 \text{ K}$ ). No information concerning the chlorine CS tensor is reported in the two previous studies; the neglect of the CS interaction will introduce errors into the determination of  $C_Q$ . The single-crystal study reports  $C_Q(^{35}\text{Cl})$  as  $4.10 \text{ MHz}$  and  $\eta$  as  $0.67$ , with errors in the tensor elements of less than  $5\%$ .<sup>8</sup> These values lie slightly outside the error limits on our values of  $4.04 \pm 0.03$  and  $0.62 \pm 0.02$ , but nevertheless the agreement is quite good. The powder NQR study reports a quadrupolar frequency,  $(e^2qQ/2h)(1 + \eta^2/3)^{1/2}$ , of  $2.160 \text{ MHz}$  for  $^{35}\text{Cl}$ .<sup>70</sup> To extract  $C_Q$  (equivalent to  $e^2qQ/h$ ), we must make an assumption regarding the asymmetry parameter. Employing values ranging from  $0.62$  to  $0.67$  results in  $C_Q(^{35}\text{Cl})$  values of  $4.067$  to  $4.029 \text{ MHz}$ , in excellent agreement with the value obtained in the present work. It is important to note that temperature effects are likely to contribute to the slight discrepancies between the three studies. In fact, Erge et al. determined a temperature dependence of  $-0.75 \text{ kHz K}^{-1}$  in the range  $120$ – $260 \text{ K}$  for the chlorine nuclear quadrupolar coupling constant in tris sarcosine calcium chloride.<sup>8</sup>

**(iii) Chlorine NMR as a Probe of Hydrogen Bonding Environment.** Based on the data reported herein, it is apparent that variations in the chlorine nuclear quadrupolar coupling constant are more easily measured than are variations in the chemical shift tensor. Nevertheless, it is certainly possible that the CS tensor is in fact an equally sensitive probe of the chlorine environment. For example, McDermott and co-workers have illustrated the dependence of the carbon CS tensors in amino acids upon their protonation state,<sup>71</sup> as well as the relationship between nitrogen CS tensors and hydrogen bonding in histidine and histidine-containing peptides.<sup>72</sup> Useful insights into the relative sensitivity of the chlorine chemical shift and EFG tensors to the local hydrogen bonding environment are afforded by ab initio calculations on a simple model system,  $\text{NH}_4^+\cdots\text{Cl}^-$  (Figure 6). A series of calculations at the RHF/6-311++G\*\* level has been carried out as a function of the nitrogen–chlorine separation. In particular, we focus on the span of the chlorine shift tensor and the nuclear quadrupolar coupling constant. Although the absolute values of these parameters are not significant due to the simplicity of the model system, instructive information may be obtained through the derivatives  $\partial\sigma_{\text{iso}}(\text{Cl})/\partial r$ ,  $\partial\Omega(\text{Cl})/\partial r$  and  $\partial C_Q(^{35/37}\text{Cl})/\partial r$ , where  $r$  is the nitrogen–chlorine separation. The slopes of the graphs shown in Figure 6 provide estimates of these derivatives near the equilibrium separation,  $\partial\Omega(\text{Cl})/\partial r = -111 \text{ ppm } \text{\AA}^{-1}$  and  $\partial C_Q(^{35}\text{Cl})/\partial r = -73 \text{ MHz } \text{\AA}^{-1}$ . The calculations also indicate that  $\partial\sigma_{\text{iso}}(\text{Cl})/\partial r$  is  $99 \text{ ppm } \text{\AA}^{-1}$ . A more in-depth computational study of the nuclear quadrupolar coupling constants in  $\text{NH}_4\text{Cl}$  has been

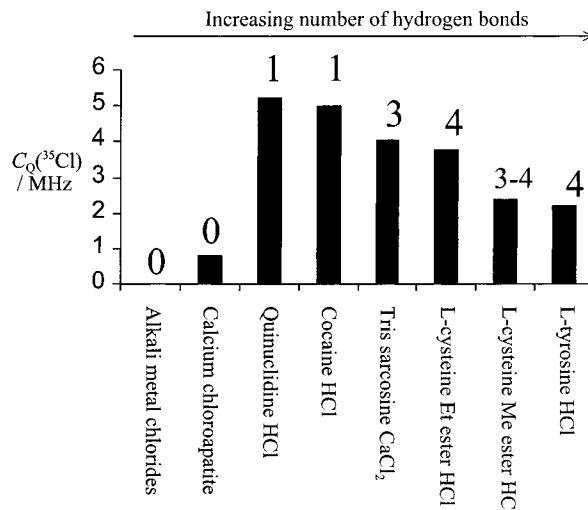


**Figure 7.** Variability in  $^{35}\text{Cl}$  nuclear quadrupolar coupling constants as a function of the total number of  $\text{N-H}\cdots\text{Cl}$ ,  $\text{O-H}\cdots\text{Cl}$ , and  $\text{S-H}\cdots\text{Cl}$  hydrogen bonds to chlorine in a series of compounds containing chloride anions.

provided by Halkier et al.<sup>73</sup> Further information is gained by examining other simple model systems in the absence of hydrogen bonding. For example, calculations on  $\text{Na}^+\cdots\text{Cl}^-$  (RHF/6-311+G\*) as a function of the sodium–chlorine distance indicate that for chlorine,  $\partial\sigma_{\text{iso}}(\text{Cl})/\partial r = 27 \text{ ppm } \text{\AA}^{-1}$ ,  $\partial\Omega(\text{Cl})/\partial r = -43 \text{ ppm } \text{\AA}^{-1}$ , and  $\partial C_Q(^{35}\text{Cl})/\partial r = -23 \text{ MHz } \text{\AA}^{-1}$ . The negative sign of  $\partial C_Q(^{35}\text{Cl})/\partial r$  for  $\text{NaCl}$  and the corresponding positive sign for  $\partial V_{\text{ZZ}}(\text{Cl})/\partial r$  (due to the negative  $Q$  for  $^{35}\text{Cl}$ ) are in agreement with higher-level calculations reported by Seth et al.<sup>74</sup> Finally, analogous calculations on a model perchlorate salt,  $\text{Na}^+\cdots\text{ClO}_4^-$ , as a function of the sodium–chlorine separation, yield values of  $\partial\sigma_{\text{iso}}(\text{Cl})/\partial r = 0.07 \text{ ppm } \text{\AA}^{-1}$ ,  $\partial\Omega(\text{Cl})/\partial r = -28 \text{ ppm } \text{\AA}^{-1}$ , and  $\partial C_Q(^{35}\text{Cl})/\partial r = 1.9 \text{ MHz } \text{\AA}^{-1}$ . Based on these calculations, it appears that in the presence of a hydrogen bond, the EFG tensor is in fact more sensitive than  $\sigma$  to changes in molecular and electronic structure around chlorine, e.g., for a change in  $r$  of  $1 \text{ \AA}$  in  $\text{NH}_4^+\cdots\text{Cl}^-$ , the change in span represents just  $7\%$  of the total chemical shift range while the change in  $C_Q(^{35}\text{Cl})$  represents nearly  $50\%$  of the total range of known  $^{35}\text{Cl}$  quadrupolar coupling constants! Notably, both derivatives for  $\text{NaClO}_4$  are much smaller than for  $\text{NH}_4\text{Cl}$ . Recently, Chapman et al. have investigated some other NMR properties of  $\text{N-H}\cdots\text{Cl}$  hydrogen bonds, e.g., the across hydrogen bond indirect nuclear spin–spin coupling constant,  $^2hJ_{\text{iso}}(^{35}\text{Cl}, ^{15}\text{N})$ , in  $\text{NH}_4\text{Cl}$  and pyridine hydrochloride using equation-of-motion coupled cluster singles and doubles (EOM-CCSD) calculations.<sup>75</sup>

Halide ions represent some of the strongest hydrogen bond acceptors.<sup>76</sup> It is generally thought that a chloride ion has the ability to bind to a maximum of four strong donors, e.g.,  $\text{O-H}$  and  $\text{N-H}$  donors.<sup>76,77</sup> Beyond this, weaker donors such as  $\text{C-H}$  may play a role. Weak  $\text{C-H}\cdots\text{Cl}$  interactions are found, for example, in quinclidine hydrochloride.<sup>29</sup> Presented in Figure 7 is a summary of chlorine quadrupolar coupling constants as a function of the total number of  $\text{N-H}\cdots\text{Cl}$ ,  $\text{O-H}\cdots\text{Cl}$ , and  $\text{S-H}\cdots\text{Cl}$  hydrogen bonds around the chloride ion in each of the compounds, as determined from the crystal structures.<sup>27–30</sup> The data shown indicate a possible trend: *as the number of hydrogen bonds to chlorine increases from one through four, the value of  $C_Q$  decreases*. An isolated chloride anion should exhibit no EFG due to its spherical symmetry; similarly a chloride ion with no opportunities for hydrogen bonding may exhibit a very small quadrupolar coupling constant, e.g.,

**TABLE 2: Comparison of Experimental and Restricted Hartree–Fock  $^{35}\text{Cl}$  NMR Parameters for L-Tyrosine Hydrochloride**

basis set on Cl	basis set on OH, $3 \times \text{NH}_3$	basis set on remaining atoms	$C_Q/\text{MHz}$	$\eta$	$\sigma_{\text{iso}}/\text{ppm}$	$\delta_{\text{iso}}/\text{ppm}$	$\Omega/\text{ppm}$	$\kappa$
6-311G	3-21G	3-21G	2.95	0.77	990.3	-16.3	84	-0.27
6-311G	6-311G	3-21G	2.68	0.59	985.4	-11.4	69	-0.10
expt. (this work)			$2.23 \pm 0.02$	$0.72 \pm 0.03$	925.7	$49.3 \pm 0.5$	< 150	

$C_Q(^{35}\text{Cl}) = 0.8 \text{ MHz}$  for calcium chloroapatite.<sup>25,78</sup> As a single hydrogen bond is added, e.g., the case of quinuclidine hydrochloride, the symmetry is distorted and a large quadrupolar coupling constant results, 5.25 MHz. This is also the case for cocaine hydrochloride, where a single  $\text{N}-\text{H}\cdots\text{Cl}$  hydrogen bond results in a  $C_Q$  of 5.027 MHz.<sup>25,79</sup> The chloride anion in tris sarcosine hydrochloride possesses three hydrogen bonds to nitrogen atoms; this results in a reduced value of  $C_Q$ , 4.04 MHz. The availability of X-ray crystal structures for the analogous compounds L-cysteine methyl ester hydrochloride and L-cysteine ethyl ester hydrochloride,<sup>28</sup> in combination with the NMR data presented in Table 1, allows for a particularly insightful analysis of the effects of the local chlorine environment on the  $^{35}\text{Cl}$  NMR parameters. The crystal structures of these two compounds are very similar, both crystallizing in the  $P2_12_12_1$  space group, and both possessing three  $\text{N}-\text{H}\cdots\text{Cl}$  bonds of comparable geometry. The only major difference reported in the structures of these compounds is the length of the  $\text{S}-\text{H}\cdots\text{Cl}$  hydrogen bond. In the methyl ester, the authors conclude that there is no significant thiol–chloride hydrogen bond, whereas in the ethyl ester, a fairly strong interaction is deduced, based on the  $\text{S}-\text{Cl}$  internuclear distances. Interpretation of the observed chlorine quadrupolar coupling parameters for these compounds in the context of the X-ray data suggests that the increased proximity of the thiol group is directly responsible for the increase in  $C_Q$  from 2.36 to 3.79 MHz; this is in agreement with the negative values of  $\partial C_Q(^{35}\text{Cl})/\partial r$  reported above for  $\text{NH}_4\text{Cl}$ . Thus, the general trend shown in Figure 7 is not strictly obeyed for these two similar compounds. However, the asymmetry parameter changes quite drastically, from 0.03 in the ethyl ester to 0.82 in the methyl ester, and may be a particularly useful parameter for comparison of the chloride sites in closely related compounds. It is also worth pointing out that point charge models indicate that the EFG at a central nucleus in coordination complexes depends on the arrangement and number of the ligands; a similar dependence likely plays an important role in determining the chlorine EFG tensor for chloride ions involved in hydrogen bonding.<sup>80,81</sup>

Neutron diffraction data are available for L-tyrosine hydrochloride.<sup>27</sup> The availability of this type of data is extremely beneficial to NMR spectroscopists owing to the high precision to which proton positions are reported. For example, the accurately known structure of L-tyrosine hydrochloride has been used recently to establish a reliable method for measuring proton–carbon distances in high-speed MAS experiments.<sup>82,83</sup> The availability of these data, including precisely known proton coordinates, has allowed us to carry out a restricted-Hartree–Fock calculation of the chlorine CS and EFG tensors. Fedotov et al. have performed density functional theory calculations of  $^{35/37}\text{Cl}$  NMR properties for some small chlorine-containing molecules.<sup>84</sup> The system for which we have carried out the calculations is shown in Figure 8a. This simplest unit incorporates the chloride anion and its four hydrogen bonding partners, i.e., four distinct tyrosine units. Incorporation of all four of these units is essential to model the hydrogen bonding environment at chlorine. The results of the calculations, summarized in Table 2, are in good agreement with the experimental data for L-tyrosine hydrochloride. The results of the second calculation,

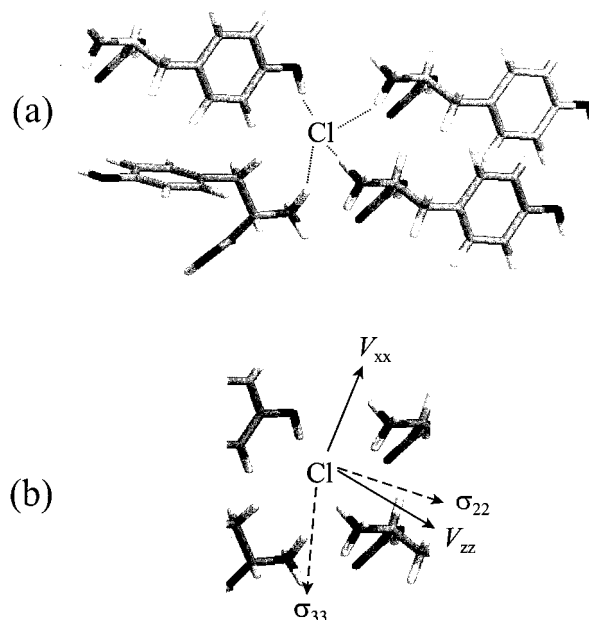


**Figure 8.** (a) Structure of L-tyrosine hydrochloride generated from the neutron diffraction atomic coordinates given in reference 27. Each chloride anion is hydrogen bonded to four protons: one from an OH group and three from different  $\text{NH}_3$  groups. (b) Detail of the structure shown in part (a), with only the atoms surrounding chlorine shown, for clarity. The calculated orientations of the chlorine nuclear magnetic shielding and electric field gradient tensors are indicated. The components shown all lie approximately in the plane of the page.  $V_{yy}$  and  $\sigma_{11}$  lie approximately perpendicular to the plane of the page.

where the 6-311G basis set has been used on the OH and  $\text{NH}_3$  groups in addition to the chloride anion, should be more reliable. The calculated quadrupolar coupling constant of 2.68 MHz is in reasonably good agreement with the experimental value of  $2.23 \pm 0.02 \text{ MHz}$ . Perhaps more important is the fact that the calculated value falls well within the experimental range for chloride anions that have four hydrogen bonds (i.e.,  $\sim 2.2\text{--}3.8 \text{ MHz}$ ). The calculations also establish that  $C_Q$  is positive; it is likely that this is true for all of experimentally determined quadrupolar coupling constants for chloride ions (Table 1 and Figure 7). Shown in Figure 8b are the calculated orientations of the nuclear magnetic shielding and EFG tensors for chlorine, with the indicated components lying approximately in the plane of the page. There is no obvious rationalization for the calculated orientation; for example, no component lies directly along one of the hydrogen bonds. Clearly, further experimental and theoretical work will be required to determine the relationship between the tensor orientations and variations in hydrogen bonding environment. To obtain credible results it is imperative that the hydrogen atom positions are known accurately.

Based on the data presented in Table 2, the span of the CS tensor is calculated to a reasonable accuracy, and the isotropic chemical shift falls in the approximate range known for chloride ions. The calculated isotropic chemical shifts are approximately 60–65 ppm less than the experimental value of 48.3 ppm. While such a discrepancy may seem large, especially given the small range of chemical shifts observed for the various compounds studied herein ( $\sim 45 \text{ ppm}$ ), it is important to recognize that the



total chlorine chemical shift range for diamagnetic compounds is nearly 1500 ppm. Thus, the 60 ppm difference between the calculated and experimental chemical shifts represents only 4% of the possible shift range. Furthermore, gas-to-solid shifts are expected to be on this order of magnitude, e.g., the shift induced on going from HCl(g) to HCl dissolved in chloropentanes is 45 ppm.<sup>47</sup>

## Conclusions

The present work has established the viability of studying solid organic hydrochloride salts using high-field <sup>35/37</sup>Cl NMR techniques. For compounds with quadrupolar coupling constants of less than ~4 MHz, magic-angle spinning at 10–15 kHz on an 18.8 T magnet allows for the acquisition of high-quality central-transition spectra with well-defined line shapes. Higher MAS rates and field strengths will facilitate <sup>35/37</sup>Cl MAS NMR studies for a wider range of compounds; analyses of both <sup>35</sup>Cl and <sup>37</sup>Cl spectra are beneficial for increasing the precision and accuracy of the chlorine NMR parameters. Acquisition of chlorine static echo and QCPMG spectra for hydrochloride salts at 18.8 T is practical. Although ab initio calculations indicate that both the CS and EFG tensors are indicative of the chlorine environment, the nuclear quadrupolar coupling constant represents the more sensitive and extractable probe. In particular, the chlorine nuclear quadrupolar coupling constant has been found to be very characteristic of the hydrogen bonding environment of the chloride ion. Further work on how the magnitude and orientation of the EFG tensor depends on the nature of the hydrogen bond donors would be beneficial. Given the range of chlorine quadrupolar coupling constants determined for the hydrochloride salts studied herein, 2.23–5.25 MHz, high-field <sup>35/37</sup>Cl MQMAS studies may be feasible for examining materials with nonequivalent chloride ion sites. Precise determinations of the chlorine chemical shift tensor and its orientation with respect to the EFG tensor are difficult for the compounds discussed in this work due to the small spans which seem to be characteristic of hydrochloride salts. Anisotropic chlorine nuclear magnetic shielding has been observed from a powder sample for the first time, in L-cysteine ethyl ester hydrochloride.

**Note Added in Proof:** Direct measurement of the <sup>35</sup>Cl chemical shift of solid NaCl with respect to a very dilute solution of NaCl in H<sub>2</sub>O has provided an improved conversion factor (cf. eq 6) of –45.37 ppm rather than –46.34 ppm. We thank Dr. Tom Nakashima for this measurement. The chemical shifts in Table 1 have been adjusted to reflect this difference.

**Acknowledgment.** The authors thank the solid-state NMR group at the University of Alberta, and Dr. Mike Lumsden and Brian Millier at Dalhousie University for many helpful comments and technical assistance. Dr. Bob McDonald is thanked for database searches for X-ray crystal structures. Part of this research was performed in the Environmental Molecular Sciences Laboratory (a national scientific user facility sponsored by the U.S. DOE Office of Biological and Environmental Research) located at Pacific Northwest National Laboratory, operated by Battelle for the DOE. We thank Nancy Isern, Andrew Lipton, Jesse Sears, Joe Ford, and David Hoyt for their assistance with the 18.8 T NMR system. We acknowledge Prof. N. Chr. Nielsen and co-workers for making available the SIMPSON program. We thank the Natural Sciences and Engineering Research Council (NSERC) of Canada for research grants. Some spectra (9.4 T) were acquired at the Atlantic Region Magnetic Resonance Centre, which is supported by NSERC. D.L.B. and M.G. thank NSERC, Dalhousie University,

the Izaak Walton Killam Trust, and the Walter C. Sumner Foundation for post-graduate scholarships. R.E.W. is a Canada Research Chair in Physical Chemistry at the University of Alberta.

## References and Notes

- Freude, D.; Haase, J. *NMR Basic Princ. Prog.* **1993**, 29, 1.
- Smith, M. E. *Annu. Rep. NMR Spectrosc.* **2001**, 43, 121.
- Smith, M. E.; van Eck, E. R. H. *Prog. Nucl. Magn. Reson. Spectrosc.* **1999**, 34, 159.
- (a) Cummins, P. L.; Bacskey, G. B.; Hush, N. S. *J. Chem. Phys.* **1987**, 87, 416. (b) Kellö, V.; Sadlej, A. J. *Chem. Phys. Lett.* **1990**, 174, 641. (c) Pyykkö, P. Z. *Naturforsch.* **1992**, 47a, 189.
- Lovas, F. J.; Tiemann, E. *J. Phys. Chem. Ref. Data* **1974**, 3, 609 (see page 661).
- Kawamori, A.; Itoh, J. *J. Phys. Soc. Jpn.* **1963**, 18, 1614.
- Spiess, H. W.; Sheline, R. K. *J. Chem. Phys.* **1971**, 54, 1099.
- Erge, Th.; Michel, D.; Petersson, J.; Windsch, W. *Phys. Status Solidi, A* **1989**, 114, 705.
- Bastow, T. J.; Stuart, S. N. *J. Phys.: Condens. Matter* **1989**, 1, 4649.
- Holzer, K.-P.; Häcker, U.; Petersson, J.; Michel, D.; Kluthe, S. *Solid State Commun.* **1995**, 94, 275.
- Jurga, S.; Seliger, J.; Blinc, R.; Spiess, H. W. *Phys. Lett. A* **1986**, 116, 295.
- Jurga, S.; Harbison, G. S.; Blümich, B.; Spiess, H. W.; Fujara, F.; Olinger, A. *Ber. Bunsen-Ges. Phys. Chem.* **1986**, 90, 1153.
- Furukawa, Y.; Ikeda, R. *Ber. Bunsen-Ges. Phys. Chem.* **1993**, 97, 1143.
- Ono, H.; Ishimaru, S.; Ikeda, R.; Ishida, H. *Chem. Phys. Lett.* **1997**, 275, 485.
- Ono, H.; Ishimaru, S.; Ikeda, R.; Ishida, H. *Bull. Chem. Soc. Jpn.* **1999**, 72, 2049.
- Skibsted, J.; Jakobsen, H. J. *Inorg. Chem.* **1999**, 38, 1806.
- Kanda, T. *J. Phys. Soc. Jpn.* **1955**, 10, 85.
- Weeding, T. L.; Veeman, W. S. *J. Chem. Soc., Chem. Commun.* **1989**, 946.
- Lefebvre, F. *J. Chim. Phys.* **1992**, 89, 1767.
- Jelinek, R.; Stein, A.; Ozin, G. A. *J. Am. Chem. Soc.* **1993**, 115, 2390.
- Bastow, T. J.; Stuart, S. N.; McDugle, W. G.; Eachus, R. S.; Spaeth, J. M. *J. Phys.: Condens. Matter* **1994**, 6, 8633.
- Becker, K. D. *J. Chem. Phys.* **1978**, 68, 3785.
- Kirkpatrick, R. J.; Yu, P.; Hou, X.; Kim, Y. *Am. Mineral.* **1999**, 84, 1186.
- Hattori, M.; Onoda, Y.; Erata, T.; Smith, M. E.; Hattori, M.; Ohki, H.; Ikeda, R. *Z. Naturforsch.* **1994**, 49a, 291.
- Yesinowski, J. P.; Buess, M. L.; Garroway, A. N.; Ziegeweid, M.; Pines, A. *Anal. Chem.* **1995**, 67, 2256.
- Lucken, E. A. C. *Nuclear Quadrupole Coupling Constants*, Academic Press: London, 1969.
- Frey, M. N.; Koetzle, T. F.; Lehmann, M. S.; Hamilton, W. C. *J. Chem. Phys.* **1973**, 58, 2547.
- Görbitz, C. H. *Acta Chem. Scand.* **1989**, 43, 871.
- Kurahashi, M.; Engel, P.; Nowacki, W. Z. *Kristallogr.* **1980**, 152, 147.
- Ashida, T.; Bando, S.; Kakudo, M. *Acta Crystallogr.* **1972**, B28, 1560.
- Hahn, E. L. *Phys. Rev.* **1950**, 80, 580.
- Chan, J. C. C. *Concepts Magn. Reson.* **1999**, 11, 363.
- (a) Carr, H. Y.; Purcell, E. M. *Phys. Rev.* **1954**, 94, 630. (b) Meiboom, S.; Gill, D. *Rev. Sci. Instrum.* **1958**, 29, 688.
- Cheng, J. T.; Ellis, P. D. *J. Phys. Chem.* **1989**, 93, 2549.
- Larsen, F. H.; Jakobsen, H. J.; Ellis, P. D.; Nielsen, N. *Chr. J. Phys. Chem. A* **1997**, 101, 8597.
- Larsen, F. H.; Jakobsen, H. J.; Ellis, P. D.; Nielsen, N. *Chr. J. Magn. Reson.* **1998**, 131, 144.
- Larsen, F. H.; Lipton, A. S.; Jakobsen, H. J.; Nielsen, N. *Chr. J. Ellis, P. D. J. Am. Chem. Soc.* **1999**, 121, 3783.
- Larsen, F. H.; Skibsted, J.; Jakobsen, H. J.; Nielsen, N. *Chr. J. Am. Chem. Soc.* **2000**, 122, 7080.
- Bryce, D. L.; Wasylishen, R. E.; Gee, M. *J. Phys. Chem. A* **2001**, 105, 3633.
- Bryce, D. L.; Wasylishen, R. E. *J. Phys. Chem. A* **1999**, 103, 7364.
- Samoson, A. *Chem. Phys. Lett.* **1985**, 119, 29.
- Mason, J. *Solid State Nucl. Magn. Reson.* **1993**, 2, 285.
- VNMR, Version 6.1B, Varian Inc., 1998.
- NUTS-NMR Utility Transform Software for Windows 95/NT, 2D Version, Acorn NMR, 1998.
- WIN-NMR, Version 6.0, Copyright Bruker-Franzen Analytik GmbH.



- (46) Hayashi, S.; Hayamizu, K. *Bull. Chem. Soc. Jpn.* **1990**, *63*, 913.
- (47) Gee, M.; Wasylishen, R. E.; Laaksonen, A. *J. Phys. Chem. A* **1999**, *103*, 10805.
- (48) Loewenstein, A.; Shporer, M.; Lauterbur, P. C.; Ramirez, J. E. *J. Chem. Soc., Chem. Commun.* **1968**, 214.
- (49) Eichele, K.; Wasylishen, R. E. *WSOLIDS NMR Simulation Package*, Version 1.17.26, 2000.
- (50) Alderman, D. W.; Solum, M. S.; Grant, D. M. *J. Chem. Phys.* **1986**, *84*, 3717.
- (51) Bak, M.; Rasmussen, J. T.; Nielsen, N. Chr. *J. Magn. Reson.* **2000**, *147*, 296.
- (52) Frisch, M. J.; Trucks, G. W.; Schlegel, H. B.; Scuseria, G. E.; Robb, M. A.; Cheeseman, J. R.; Zakrzewski, V. G.; Montgomery, J. A., Jr.; Stratmann, R. E.; Burant, J. C.; Dapprich, S.; Millam, J. M.; Daniels, A. D.; Kudin, K. N.; Strain, M. C.; Farkas, O.; Tomasi, J.; Barone, V.; Cossi, M.; Cammi, R.; Mennucci, B.; Pomelli, C.; Adamo, C.; Clifford, S.; Ochterski, J.; Petersson, G. A.; Ayala, P. Y.; Cui, Q.; Morokuma, K.; Malick, D. K.; Rabuck, A. D.; Raghavachari, K.; Foresman, J. B.; Cioslowski, J.; Ortiz, J. V.; Stefanov, B. B.; Liu, G.; Liashenko, A.; Piskorz, P.; Komaromi, I.; Gomperts, R.; Martin, R. L.; Fox, D. J.; Keith, T.; Al-Laham, M. A.; Peng, C. Y.; Nanayakkara, A.; Gonzalez, C.; Challacombe, M.; Gill, P. M. W.; Johnson, B. G.; Chen, W.; Wong, M. W.; Andres, J. L.; Head-Gordon, M.; Replogle, E. S.; Pople, J. A. *Gaussian 98*, revision A.7; Gaussian, Inc.: Pittsburgh, PA, 1998.
- (53) Levy, H. A.; Peterson, S. W. *Phys. Rev.* **1952**, *86*, 766.
- (54) Strømme, K. O. *Acta Chem. Scand.* **1974**, *A28*, 515.
- (55) Braekken, H.; Harang, L. Z. *Kristallogr.* **1930**, *75*, 538.
- (56) Huber, K. P.; Herzberg, G. Constants of Diatomic Molecules (data prepared by Gallagher, J. W., Johnson, R. D., III) in *NIST Chemistry WebBook, NIST Standard Reference Database Number 69*; Mallard, W. G., Linstrom, P. J., Eds.; National Institute of Standards and Technology: Gaithersburg, MD, 2000 (<http://webbook.nist.gov>).
- (57) (a) Ditchfield, R. *Mol. Phys.* **1974**, *27*, 789. (b) Wolinski, K.; Hinton, J. F.; Pulay, P. *J. Am. Chem. Soc.* **1990**, *112*, 8251.
- (58) (a) Chesnut, D. B.; Moore, K. D. *J. Comput. Chem.* **1989**, *10*, 648. (b) Chesnut, D. B.; Rusiloski, B. E.; Moore, K. D.; Egolf, D. A. *J. Comput. Chem.* **1993**, *14*, 1364.
- (59) Mills, I.; Cvitaš, T.; Homann, K.; Kallay, N.; Kuchitsu, K. *Quantities, Units and Symbols in Physical Chemistry*, 2nd ed., International Union of Pure and Applied Chemistry Physical Chemistry Division, Blackwell Science: Oxford, 1993.
- (60) Aikitt, J. W. In *Multinuclear NMR*; Mason, J., Ed.; Plenum: New York, 1987; chapter 17.
- (61) Lindman, B.; Forsén, S. *NMR Basic Princ. Prog.* **1976**, *12*, 1.
- (62) Fabricant, B.; Muentner, J. S. *J. Chem. Phys.* **1977**, *66*, 5274.
- (63) (a) Medek, A.; Harwood, J. S.; Frydman, L. *J. Am. Chem. Soc.* **1995**, *117*, 12779. (b) Medek, A.; Frydman, L. *J. Braz. Chem. Soc.* **1999**, *10*, 263.
- (64) Jäger, C. *NMR Basic Princ. Prog.* **1994**, *31*, 133.
- (65) Skibsted, J.; Nielsen, N. C.; Bildsøe, H.; Jakobsen, H. J. *J. Magn. Reson.* **1991**, *95*, 88.
- (66) Malli, G.; Fraga, S. *Theor. Chim. Acta* **1966**, *5*, 275.
- (67) Wigand, S.; Weiden, N.; Weiss, A. *Ber. Bunsen-Ges. Phys. Chem.* **1989**, *93*, 913.
- (68) Nakamura, N.; Chihara, H. *J. Phys. Soc. Jpn.* **1967**, *22*, 201.
- (69) Eichele, K.; Wasylishen, R. E.; Grossert, J. S.; Olivieri, A. C. *J. Phys. Chem.* **1995**, *99*, 10110.
- (70) Blinc, R.; Mali, M.; Osredkar, R.; Seliger, J. *J. Chem. Phys.* **1975**, *63*, 35.
- (71) Gu, Z.; McDermott, A. *J. Am. Chem. Soc.* **1993**, *115*, 4282.
- (72) Wei, Y.; de Dios, A. C.; McDermott, A. E. *J. Am. Chem. Soc.* **1999**, *121*, 10389.
- (73) Halkier, A.; Jaszuński, M.; Jørgensen, P. *Phys. Chem. Chem. Phys.* **1999**, *1*, 4165.
- (74) Seth, M.; Pernpointer, M.; Bowmaker, G. A.; Schwerdtfeger, P. *Mol. Phys.* **1999**, *96*, 1767.
- (75) Chapman, K.; Crittenden, D.; Bevirt, J.; Jordan, M. J. T.; Del Bene, J. E. *J. Phys. Chem. A* **2001**, *105*, 5442.
- (76) Desiraju, G. R.; Steiner, T. *The Weak Hydrogen Bond*, IUCr Monographs on Crystallography 9, Oxford University Press: Oxford, 1999; Section 3.3.
- (77) Jeffrey, G. A.; Saenger, W. *Hydrogen Bonding In Biological Structures*; Springer-Verlag: Berlin, 1991.
- (78) Yesinowski, J. P.; Eckert, H. unpublished data, California Institute of Technology, 1985.
- (79) Gabe, E. J.; Barnes, W. H. *Acta Crystallogr.* **1963**, *16*, 796.
- (80) Hee Han, O.; Oldfield, E. *Inorg. Chem.* **1990**, *29*, 3666.
- (81) Aikitt, J. W.; Mann, B. E. *NMR and Chemistry: An introduction to modern NMR spectroscopy*, 4<sup>th</sup> ed.; Stanley Thornes Ltd: Cheltenham, UK, 2000; pp 113–114.
- (82) van Rossum, B.-J.; de Groot, C. P.; Ladizhansky, V.; Vega, S.; de Groot, H. J. M. *J. Am. Chem. Soc.* **2000**, *122*, 3465.
- (83) van Rossum, B.-J. *Proefschrift*, Universiteit Leiden, 2000.
- (84) Fedotov, M. A.; Malkina, O. L.; Malkin, V. G. *Chem. Phys. Lett.* **1996**, *258*, 330.